Integrin-Associated CD151 Drives ErbB2-Evoked Mammary Tumor Onset and Metastasis[1,2]

Xinyu Deng[*,3], Qinglin Li[†,3], John Hoff[*,3], Marian Novak[*], Helen Yang[‡], Hongyan Jin[*], Sonia F. Erfani[*], Chandan Sharma[†], Pengcheng Zhou[†], Isaac Rabinovitz[§], Arnoud Sonnenberg[¶], Yajun Yi[#], Peter Zhou[*], Christopher S. Stipp[**], David M. Kaetzel[*], Martin E. Hemler[†] and Xiuwei H. Yang[*]

[*]Department of Molecular and Biomedical Pharmacology, Department of Molecular and Cellular Biochemistry, and Markey Cancer Center, University of Kentucky, Lexington, KY; [†]Dana-Farber Cancer Institute and Harvard Medical School, Boston, MA; [‡]Department of Materials Science and Engineering, Massachusetts Institute of Technology, Cambridge, MA; [§]Division of Cancer Biology and Angiogenesis, Department of Pathology, Beth Israel Deaconess Medical Center and Harvard Medical School, Boston, MA; [¶]Division of Cell Biology, The Netherlands Cancer Institute, Amsterdam, Netherlands; [#]Division of Genetic Medicine, Vanderbilt University, Nashville, TN; [**]Department of Biology, University of Iowa, Iowa City, IA

Abstract

ErbB2[+] human breast cancer is a major clinical problem. Prior results have suggested that tetraspanin CD151 might contribute to ErbB2-driven breast cancer growth, survival, and metastasis. In other cancer types, CD151 sometimes supports tumor growth and metastasis. However, a definitive test of CD151 effects on *de novo* breast cancer initiation, growth, and metastasis has not previously been done. We used CD151 gene–deleted mice expressing the MMTV-ErbB2 transgene to show that CD151 strongly supports ErbB2^{+} mammary tumor initiation and metastasis. Delayed tumor onset (by 70-100 days) in the absence of CD151 was accompanied by reduced survival of mammary epithelial cells and impaired activation of FAK- and MAPK-dependent pathways. Both primary tumors and metastatic nodules showed smooth, regular borders, consistent with a less invasive phenotype. Furthermore, consistent with impaired oncogenesis and decreased metastasis, CD151-targeted MCF-10A/ErbB2 cells showed substantial decreases in three-dimensional colony formation, EGF-stimulated tumor cell motility, invasion, and transendothelial migration. These CD151-dependent functions were largely mediated through $\alpha_6\beta_4$ integrin. Moreover, CD151

ablation substantially prevented PKC- and EGFR/ERK–dependent $\alpha_6\beta_4$ integrin phosphorylation, consistent with retention of epithelial cell polarity and intermediate filament cytoskeletal connections, which helps to explain diminished metastasis. Finally, clinical data analyses revealed a strong correlation between CD151 and ErbB2 expression and metastasis-free survival of breast cancer patients. In conclusion, we provide strong evidence that CD151 collaborates with LB integrins (particularly $\alpha_6\beta_4$) and ErbB2 (and EGFR) receptors to regulate multiple signaling pathways, thereby driving mammary tumor onset, survival, and metastasis. Consequently, CD151 is a useful therapeutic target in malignant ErbB2$^+$ breast cancer.

Neoplasia (2012) 14, 678–689

Introduction

Epidermal growth factor receptor 2 (ErbB2/HER2), a member of the epidermal growth factor receptor family, is amplified in 15% to 25% of human breast cancers. This potent oncogenic receptor kinase drives breast tumor development, progression, and metastasis, leading to poor patient prognosis [1–3]. Despite advances in drug treatment of ErbB2-amplified breast cancer (e.g., with trastuzumab, lapatinib), many patients fail to respond or respond initially but become resistant within 1 year [4]. Hence, the malignancy of ErbB2$^+$ breast cancer remains a significant clinical threat, and more treatment options are needed.

Extensive studies from our group and others have shown that CD151, a member of the tetraspanin protein family [5], contributes to the malignancy of human cancer [6–9]. Analyses of human breast tumor tissues have revealed significant elevation of CD151 expression in human estrogen receptor–negative (ER$^-$) tumors, which include basal-like and ErbB2$^+$ subtypes [10,11]. Further supporting clinical relevance is the marked impact of CD151 on mammary tumor growth and metastasis in xenograft studies using immunodeficient mice [8,10]. Also, ablation of CD151 markedly impaired epidermal growth factor (EGF)–mediated breast cancer cell attachment, motility, and invasion; the cross-talk between integrins and ErbB receptors; and tumor cell's sensitivity to ErbB2 antagonists [12]. Together, these results suggest that CD151 is a central player in the malignancy of human ErbB2$^+$ breast cancer and is a promising therapeutic target.

In both normal and malignant epithelial cells, CD151 is tightly linked to cell surface adhesion receptors ($\alpha_3\beta_1$, $\alpha_6\beta_1$, $\alpha_6\beta_4$), which are the laminin binding (LB) integrins [10,13,14]. CD151 physically interacts with LB integrin α_3 or α_6 subunit to form tight protein complexes through their respective extracellular domains [13]. In addition, CD151 orchestrates assembly of other tetraspanins and nontetraspanin components into large complexes on the cell surface, known as tetraspanin-enriched membrane microdomains (TEMs) [13]. Therefore, it is postulated that CD151 affects LB integrin functions and diverse cellular processes by modulating the lateral movement of these adhesion molecules and by recruiting diverse signaling molecules, including protein kinase C (PKC), into TEMs [10,13,15].

Despite more than 50 studies linking CD151 to various aspects of tumor and tumor cell behavior, two critical results have been lacking: 1) CD151 had not been shown to affect breast cancer initiation in a spontaneous (i.e., *de novo*) model and 2) the effects of CD151 on spontaneous tumor metastasis had not been analyzed. Given that CD151 functions through LB integrins (e.g., $\alpha_3\beta_1$ and $\alpha_6\beta_4$), which frequently coexist on normal and malignant epithelial cells [7], but have potentially opposing roles during tumor progression and metastasis [16–19],

one cannot predict in advance how CD151 will affect tumor initiation and metastasis.

To address definitively the roles of CD151 during *in vivo* tumor onset, growth, and metastasis, we use CD151 wild-type and knockout mice [20], combined with a spontaneous breast cancer mouse mammary tumor virus (MMTV)–c-Neu (ErbB2) tumor model [21]. Also, to gain mechanistic insight into tumor cell autonomous roles of CD151 (i.e., free of tumor-stroma complications), we carried out extensive *in vitro* functional and signaling analyses using three-dimensional cultured mammary epithelial cells as a model. Our results demonstrate that CD151 drives the onset and metastasis of ErbB2-evoked mammary tumors. Loss of CD151 markedly impaired tumor cell survival and activation of focal adhesion kinase (FAK)– and MAP kinase kinase (MEK)/extracellular signal–regulated kinase (ERK)–mediated signaling. These actions of CD151 are associated with integrin $\alpha_3\beta_1$- and $\alpha_6\beta_4$-dependent cell attachment, motility, invasion, survival, and signaling crosstalk with epidermal growth factor receptor (EGFR) and ErbB2 receptors. Overall, our studies provide the first *in vivo* evidence that CD151, a major partner of LB integrins, is a critical regulator of mammary tumor onset and metastasis, particularly in the context of ErbB2-evoked breast cancer.

Materials and Methods

Mice and In Vivo Tumor Analyses

ErbB2 transgenic FVB mice, which express multiple copies of intact rat c-Neu gene under MMTV promoter [22], were purchased from the Jackson Laboratory (Bar Harbor, ME). These mice typically form mammary tumors (in 4-10 months), and after 8 months, most mice also show tumor metastasis to lungs [22]. CD151-null mice were generated in house [20]. To enhance oncogenic susceptibility, CD151-null mice on 129SVE background were backcrossed onto the FVB background three times before being bred to ErbB2-overexpressing transgenic animals. To minimize the influence of a pathologic kidney phenotype, which may be evident in more fully inbred FVB [23,24], CD151-null mice were not backcrossed further onto the FVB background. After intercrossing between ErbB2-expressing CD151$^{+/-}$ mice, the resulting mouse littermates were transgenic for ErbB2 but varied in CD151 genotype: +/+ (WT) or +/– (Het) or –/– (KO). Attrition was minimal (<1% mice lost per year) and was not affected by CD151 genotype. All mice were housed under identical conditions, and tumors were scored blind by multiple independent individuals. Mice were independently genotyped at the beginning and end of experiments and examined twice weekly for palpable mammary tumors, and tumor sizes were measured using calipers.

At the end of *in vivo* experiments, tumor tissues, lung, and kidney were collected and stored at –80°C for biochemical analyses or fixed in 10% neutral formalin (Sigma-Aldrich, St Louis, MO) and subsequently stored in 70% ethanol before being embedded into paraffin block for subsequent hematoxylin and eosin and immunohistochemistry (IHC) analyses. Whole-mount analysis of mammary gland development was carried out essentially as described [25]. Briefly, inguinal mammary glands were surgically removed and fixed and followed by staining with Carmine solution for 1 to 2 days. The stained glands were imaged under dissecting microscope with a digital camera.

Cell Lines and Culture

Immortalized human mammary epithelial cells, MCF-10A (from ATCC, Manassas, VA) and MCF-10A/ErbB2 (provided by J. Brugge at Harvard Medical School), were maintained in medium supplemented in 5% horse serum, insulin, and EGF as previously described [10]. Three-dimensional culture of MCF-10A/ErbB2 cells was carried out essentially according to the protocol described by Debnath and Brugge [26]. In brief, cells were plated onto Matrigel-coated eight-well glass-bottom chamber slides at 5×10^4 per well in the presence of culture medium supplemented with 2% Matrigel (BD Bioscience, San Jose, CA), along with various inhibitors or stimulants. The cultured medium was replaced every second day until formation of acinar-like colonies. Mouse tumor cell lines were generated from tumor-bearing transgenic animals as described [25]. All cell cultures were carried out at 37°C under 5% CO_2.

Antibodies and Reagents

Antibodies to mouse integrins and tetraspanin proteins were obtained from BD Biosciences (San Jose, CA) or R&D Systems (Minneapolis, MN). Antibodies to human integrins and tetraspanins were raised in-house [10,27]. 1A5, an anti–human CD151 monoclonal antibody, was a gift from Dr Zijlstra, Vanderbilt University. Antibodies to cleaved caspase 3 and to total and/or phosphorylated forms of AKT, EGFR, ErbB2, ErbB3, PAK1, and ERK1/2 were obtained from Cell Signaling Technology (Danvers, MA). Antibodies against nuclear factor κB (NF-κB) and to total and/or phospho-FAK, Src, and p130CAS were from Santa Cruz Biotechnology (Santa Cruz, CA). Antibodies recognizing phospho-serine residues in the β$_4$ cytoplasmic tail were described elsewhere [27,28]. Antibody for Ki-67 was obtained from Thermo-Fisher Scientific (Waltham, MA). Doxorubicin was obtained from Sigma-Aldrich. FAK inhibitor (TAE-266) was a gift from Novartis (Boston, MA). Inhibitors of the MEK/ERK pathway (U0126) and EGFR and ErbB2 (lapatinib) were obtained from LC Laboratories (Woburn, MA).

In Vitro *Cell Function Assays*

Static cell adhesion assays were carried out as described [15,29]. Briefly, semiconfluent cells were rinsed three times in phosphate-buffered saline and detached using dissociation buffer (Invitrogen, Carlsbad, CA), labeled with fluorescent dye, and then plated on laminin-coated 96-well plates at 3×10^4 per well. After 45 minutes, nonadherent cells were removed, and percent cell attachment was determined based on fluorescence quantitation. Cell invasion was carried out using a Matrigel-coated Boyden chamber in the presence of 10 ng/ml of EGF. Tumor cells seeded at 1×10^5 per well were allowed to invade for 17 to 20 hours before quantitation as described [10]. For measurement of random cell motility, cells were seeded onto 24-well plates at 1.5×10^4 per well, placed into an OKALAB incubator

(equipped with a heater and gas mixer), and maintained at 37°C and 5% CO_2. Images were obtained with a Nikon Automated Eclipse Ti-E inverted microscope (Nikon Instruments, Inc, Melville, NY) at 20-minute intervals for 12 hours, and cell movement distance was quantified using Nikon NIS Elements Advanced Analysis Software (Nikon Instruments, Inc). For assessing transendothelial cell migration, 5-μm pore polycarbonate transwell inserts were placed in 24-well plates (Costar, Milpitas, CA) that had been precoated with a layer of Matrigel (BD Biosciences). Then, human umbilical vein endothelial cells (Lonza, Walkersville, MD) were grown to a confluent monolayer, and dye-labeled epithelial cells were seeded at 2×10^5 per well and allowed to migrate for 6 hours at 37°C. Motile cells were stained and quantified using the Nuance multispectral imaging system (Caliper Life Sciences, Hopkinton, MA). Colony formation by mammary epithelial cells under three-dimensional culture was assayed as described [26]. Size and quantities of acinar-like colonies were determined using Nikon NIS-Elements Advanced Analysis Software.

Transfection, Flow Cytometry, Immunofluorescence, and IHC Analyses

Stable knockdown of more than 90% of CD151 proteins in MCF-10A and MCF-10A/ErbB2 cells was carried out as previously described [10] and confirmed by flow cytometry or Western blot analysis with anti-CD151 monoclonal antibodies (5C11 and 1A5). For re-expression analyses, intact CD151 and an extracellular domain mutant (lacking integrin association [30]) were introduced into cells by using retroviral infection and selected with 100 μg/ml Zeocin (Invitrogen). The expression of cell surface molecules was analyzed by flow cytometry or by immunofluorescence staining of live cells grown under three-dimensional conditions and imaged under a confocal microscope. To detect intracellular proteins, cells were fixed and then stained with antibodies [10] and visualized under a confocal microscope. IHC analyses were carried out as previously described [10]. After antigen retrieval, tumor sections were consecutively stained with primary antibodies and biotin-conjugated secondary antibodies, followed by incubation with Avidin and detection (DAB kit; BD Biosciences).

Analyses of Signaling, Co-immunoprecipitation, and Immunoblot Analysis

For signaling analyses, cells were seeded onto six-well plates at 2×10^5 cells per well. After overnight starvation, cells were stimulated and lysed in RIPA buffer [10,12] supplemented with 1 mM NaV_3O_4 and protease inhibitor cocktail. For examination of CD151 association with integrin proteins, mouse tumor cells were radiolabeled with [^{3}H]-palmitate, lysed in buffer containing 1% Brij-96, and then immunoprecipitated with the indicated monoclonal antibodies, and radiographic detection was as previously described [29,31]. For tissue analyses, frozen tumor tissues were weighed and homogenized in ice-cold 1:5 (vol/vol) RIPA buffer. Protein concentrations were measured using DC Protein Determination Kit (Bio-Rad, Hercules, CA). Equal amounts of proteins were separated on SDS-PAGE, transferred onto nitrocellulose membrane, and then blotted with the indicated antibodies. For each set of samples shown, proteins have been run, blotted, and examined on the same gel and the same membrane.

## Analysis of Metastasis-Free Survival of Breast Cancer Patients

Single-gene (*CD151* alone, *ErbB2* alone) and two-gene (*CD151* and *ErbB2*) signature-based analyses were conducted on multiple independent human breast cancer data sets. The binary group assignments

for each patient sample were determined on the basis of first bifurcation of the clustering dendrograms [32].

Results

Disruption of CD151 Delays the Onset of ErbB2-Evoked Mammary Tumors in Mice

To evaluate the contribution of CD151 to ErbB2-evoked mammary tumorigenesis *in vivo*, mouse littermates expressing ErbB2 and various CD151 genotypes were examined for initial tumor appearance and growth over 420 days. As shown (Figure 1*A*), deletion of single (CD151$^{+/-}$) or both (CD151$^{-/-}$) alleles led to a significant delay in tumor onset (102 and 69 days, respectively). However, deletion of CD151 seemed to minimally influence tumor growth rate monitored during a 3-week interval (Figure 1*B*). Also, CD151 removal did not alter
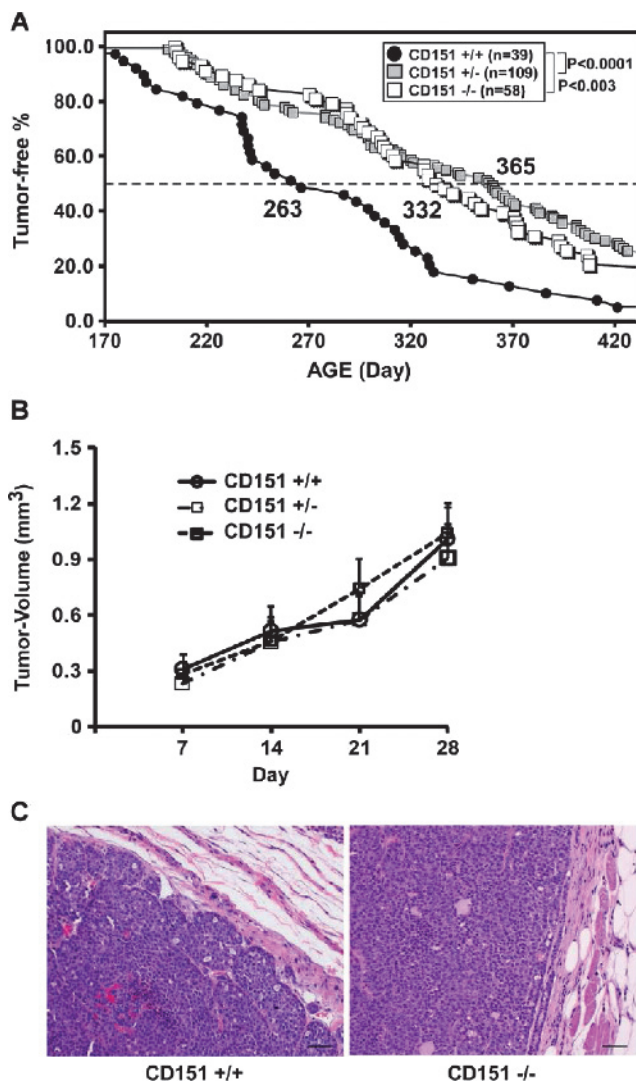
Figure 1. Impact of CD151 removal on ErbB2-induced mammary tumorigenesis. (A) Kaplan-Meier plots for tumor-free survival comparing mice with varying CD151 genotypes. The median time to tumor onset (in days) is shown. (B) Tumor volume (mean ± SEM) over time, starting with initial tumor detection, is indicated for tumor-bearing mice (for each group, $n = 15$). (C) Representative images of hematoxylin and eosin–stained primary tumor sections prepared from a total of 20 to 25 mice per CD151 genotype. Scale bar, 100 μm.
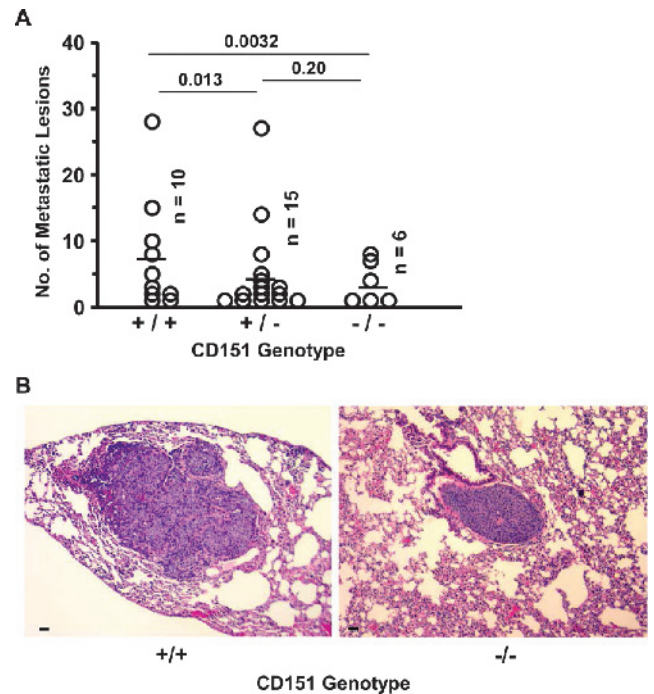
Figure 2. CD151 deletion and pulmonary metastasis. (A) Numbers of pulmonary lesions per mouse, plus average values, are indicated. Differences were assessed using nonparametric Kruskal-Wallis test; P values are indicated. Numbers of mice with pulmonary metastasis are indicated for each CD151 genotype. (B) Typical hematoxylin and eosin–stained sections of pulmonary lesions from wild-type and null tumor-bearing mice. Scale bar, 100 μm.

the extent of tumor vascularization (data not shown). In addition, multiplicity of mammary tumors remained unaffected, with less than 5% of the animals developing more than one tumor over the course of the experiment (data not shown), as expected for mice expressing the intact ErbB2/c-*neu* transgene [22]. Moreover, tumors from CD151$^{+/+}$ mice (Figure 1*C*) exhibited solid nodular structures, extensive stromal infiltrates, and protruding borders [33]. In contrast, these morphologic features were less apparent in most tumors derived from CD151$^{-/-}$ mice, largely resembling those of noninvasive ductal carcinoma *in situ* [34].

CD151 Promotes Spontaneous Metastasis of ErbB2-Induced Mammary Tumors

Next, we assessed the impact of CD151 deletion on spontaneous pulmonary metastasis in ErbB2 transgenic mice. To exclude effects of tumor burden, lungs were collected from mice only after primary tumors had reached ~4.2 cm³ in size. The number of metastatic lesions per lung in wild-type mice (~7.5/lung) was significantly reduced in CD151$^{+/-}$ (~4/lung) and CD151$^{-/-}$ mice (~2/lung) (Figure 2*A*). Furthermore, the morphologies of metastatic lesions differed markedly between these groups. Whereas lesions from CD151$^{+/+}$ mice were multifocal, nodular, and characterized by extensive stromal infiltration, those from CD151$^{-/-}$ mice were more sheet-like and reminiscent of morphologies seen in less invasive mammary tumors (Figure 2*B*). With loss of CD151 alleles, there was also a trend toward reduced incidence of pulmonary metastases (Figure W1*A*), and the average size of metastatic lesions in CD151$^{+/-}$ and CD151$^{-/-}$ mice was 44% to 51% of that in CD151$^{+/+}$ mice (Figure W1*B*).

Although CD151-het mice showed substantially delayed tumor initiation and reduced metastasis, there was no evidence for kidney

pathology in the 109 CD151-het mice analyzed. Among the 58 CD151-null mice analyzed, none showed loss of body weight or any other visual evidence for poor health, during nearly 2 years of monitoring. However, on inspection of the kidneys, 3 of 58 mice did show apparent kidney pathology (Figure W2) similar to that previously described [23].

Impaired Tumor Onset in CD151-null Mice Is Associated with Decreased Cell Survival and Signaling

To gain mechanistic insight into the role of CD151 in tumor onset, proliferation and survival were analyzed. CD151 deletion caused little change in the number of primary tumor cells positive for proliferation marker Ki-67 (Figure 3A, *left panels*). In contrast, the number of cleaved caspase 3–positive cells in CD151-deficient tumors was significantly increased compared with wild-type ($P < .05$; Figure 3, *right panels*). Relative to total cells analyzed, the extent of survival decreased 6.0% (7.5% – 1.5%).

To understand mechanisms by which CD151 may support epithelial cell survival, changes in ErbB2-mediated signaling pathways were analyzed in four representative individual tumor samples derived from each of CD151 wild-type and null groups. As indicated (Figure 4A), there was minimum consistent change in total or phosphorylated levels

A Ki-67   Caspase 3

B
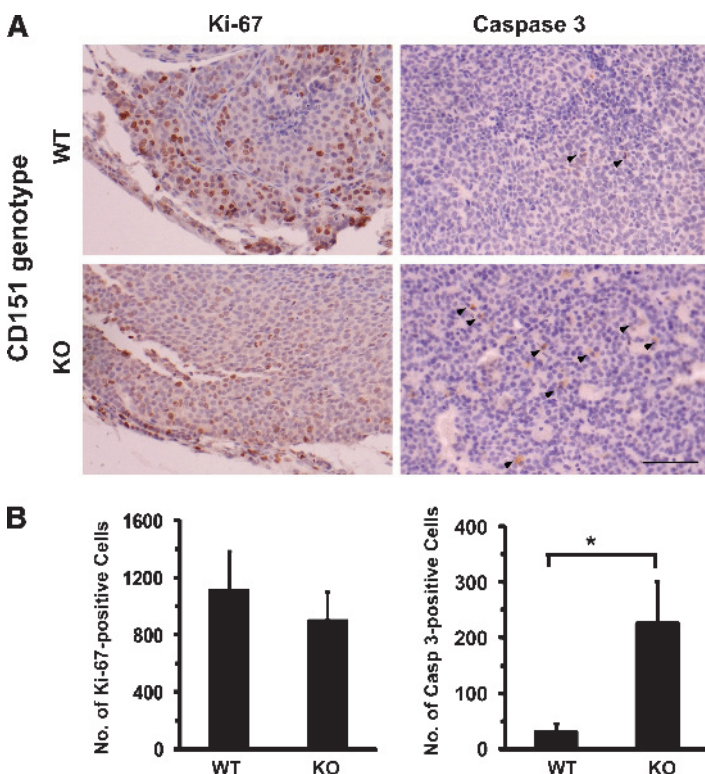
Figure 3. Effects of CD151 deletion on primary tumor proliferation and survival. (A) IHC analyses of sections of primary tumors from CD151 wild-type (WT) and null (KO) mice: (a and c) staining for Ki-67; (b and d) for caspase 3. Arrowheads indicate caspase 3–positive cells. (B) Quantitation of Ki-67 and caspase 3–positive cells (mean ± SEM). Numbers of positive cells per area were calculated for $n = 5$ mice for each CD151 genotype. Cleaved caspase 3–positive cells represent 1.5% and 7.5% of total cells in areas counted for WT and KO mice, respectively. Scale bar, 100 μm.
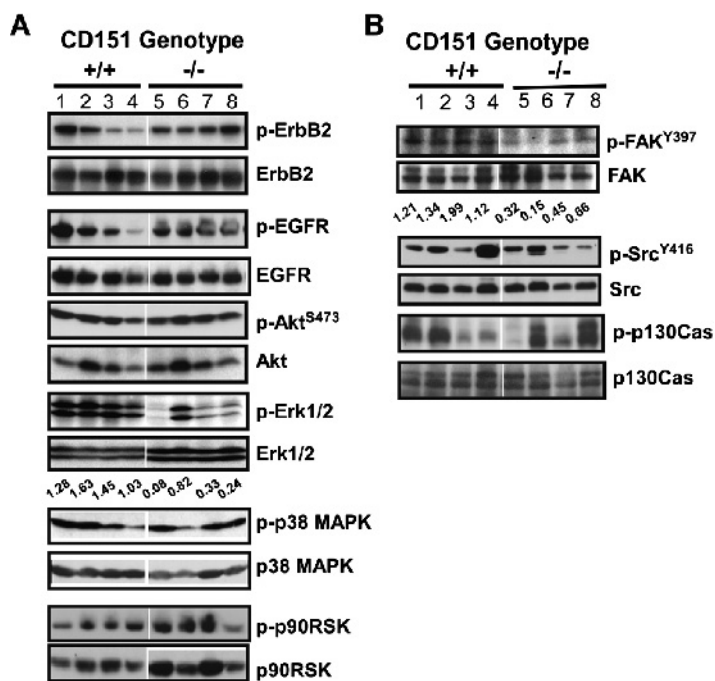
Figure 4. Loss of CD151 impairs signaling in mouse mammary tumors. (A) Lysates were prepared from four representative individual tumors from CD151 +/+ and −/− mice and blotted with indicated antibodies. The numbers below ERK1/2 and FAK represent phosphorylated/total protein ratios from densitometry measurements. Activation of ErbB2 and EGFR and their major downstream effectors was determined by blot analysis with antibodies recognizing Y1221/1222 of ErbB2, S473 of Akt, and T202/Y204 of ERK. (B) Changes in integrin-mediated tyrosine phosphorylation cascade. Phosphorylation of FAK and Src was detected using antibodies recognizing Y397 of FAK, Y416 of Src, and p130Cas, respectively. Results are representative of multiple independent analyses.

of ErbB2, EGFR, or AKT in primary tumors, in agreement with our prior studies of CD151 in human ER$^-$ breast cancer cells [10,12]. However, activation of ERK, a critical downstream effector of ErbB2 and integrin signaling, was markedly decreased when CD151 was deleted (Figure 4A, *compare lanes 5-8 with lanes 1-4*). Despite diminished activation of ERK, there was little change in activation of p90RSK (a downstream effecter of ERK, which can mediate survival [35,36]) or p38 MAPK (an alternate pathway to ERK; Figure 4A). Activation of FAK, a pivotal downstream effector of integrin signaling, was also markedly diminished, as evidenced by reduced Y397 phosphorylation (Figure 4B, *lanes 5-8*). By contrast, there were minimal changes in phosphorylation of c-Src (at Y416) or p130Cas (at Y410), despite both being linked to integrin signaling [7].

CD151 and Mammary Gland Development

Many of the same molecules that regulate mammary gland development also are involved in breast tumorigenesis [37–39]. Hence, three pairs of ErbB2-expressing mouse littermates of varying CD151 genotypes were subjected to whole-mount analyses of mammary glands. As shown (Figure W3), outgrowth of mammary glands was only a little altered depending on the presence or absence of CD151 in ErbB2$^+$ mice. Secondary branches appeared to show a small increase in number accompanied by a reduction in length in CD151-null mice. Similar
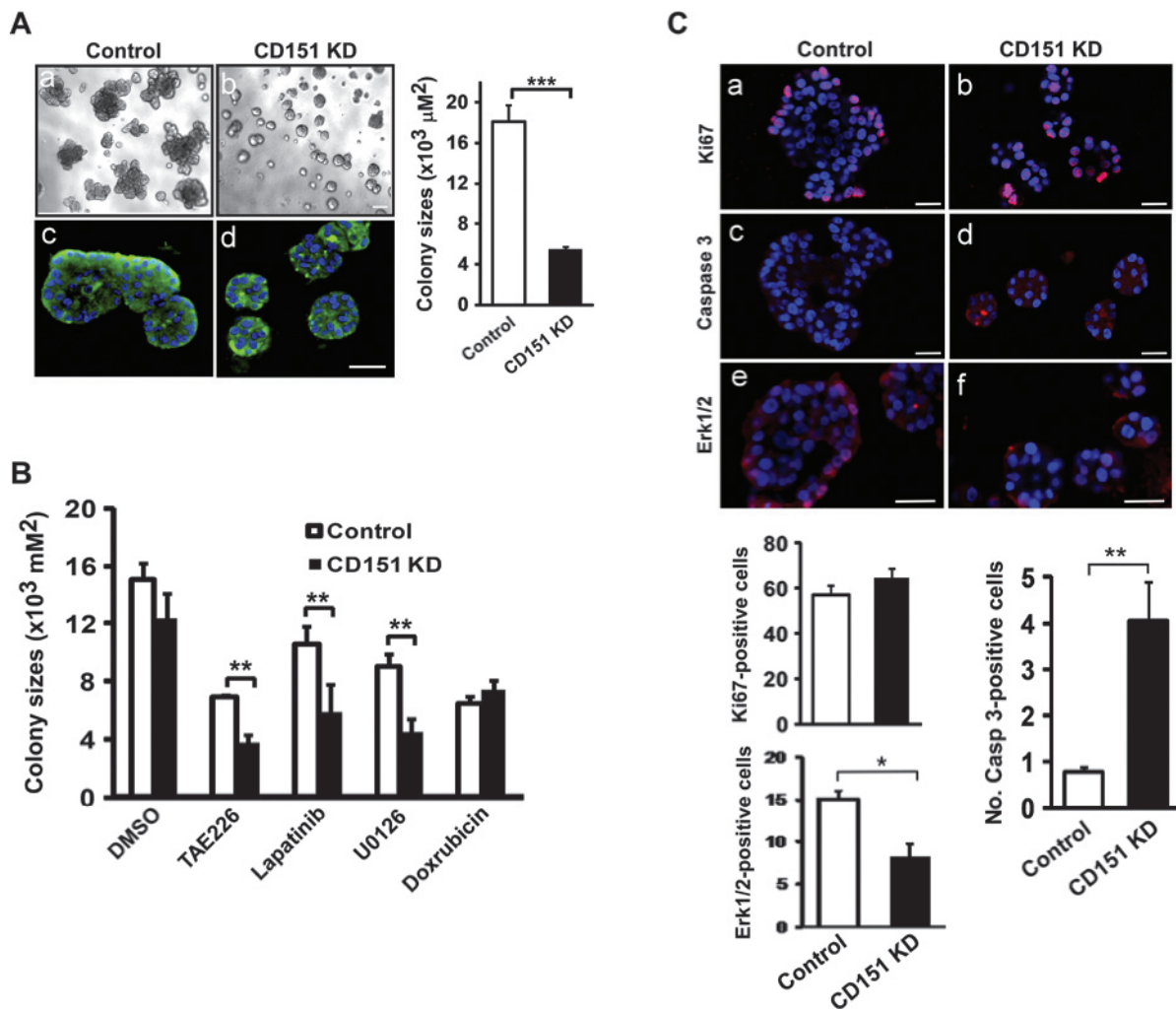
Figure 5. Ablation of CD151 decreases survival of MCF-10A/ErbB2 cells cultured in three dimensions. (A) Images of acinar-like structures are shown for cells expressing control short hairpin RNA (shRNA) (a, c) or CD151 shRNA (b, d) after 5 days of three-dimensional culture. Top panel: Representative fields were visualized using a phase-contrast microscope (a, b) and by confocal immunofluorescence imaging of antibody-stained colonies (c, d). Blue indicates DAPI staining of nuclei; green, antibody staining for smooth muscle actin (SMA). Scale bar, 50 μm. Right panel: Average colony areas in multiple random fields (mean ± SEM, $n = 3$). (B) Inhibition of acinar-like colony formation (mean ± SEM, $n = 3$). Three days after treatment with 0.5 μM lapatinib, 1.0 μM TAE266, 2.0 μM U0126, or 0.5 μM doxorubicin, colonies were imaged and quantitated. (C) Immunofluorescence analyses were carried out with indicated antibodies or DAPI for nuclear visualization. Confocal images of stained colonies: cells expressing control shRNA (a, c, e); CD151 shRNA (b, d, f). Staining for Ki-67 (a and b); caspase 3 (c and d); ERK1/2 (e and f). Blue indicates DAPI staining; red, antibody staining. Scale bar, 50 μm. Bottom panel: Percentages of positively stained cells (mean ± SEM; $n = 3$). All data are representative of multiple experiments. *$P < .05$, **$P < .01$, ***$P < .001$.

differences were also noted for CD151-null mice in the absence of *ErbB2* oncogene (data not shown).

Recapitulation of In Vivo *CD151 Functions Using* In Vitro *Cultured Mammary Epithelial Cells*

To examine the effects of CD151 in a cell-autonomous system (i.e., no possible contributions from tumor microenvironment), we used MCF-10A/ErbB2 cells in three-dimensional cell culture. In this system, differences in size and morphology of colonies reflect tumor-forming capability of ErbB2-driven carcinoma cells [40–42]. Whereas control cells formed typical ErbB2-driven disorganized colonies under three-dimensional culture [40], CD151 ablation by RNAi not only markedly decreased colony size but also partially restored acini integrity in a 5-day assay (Figure 5*A*, *b* and *d*).

To reinforce conclusions from Figure 4, we next assessed the extent to which CD151 synergizes with ErbB2-driven FAK and ERK pathways to enhance colony size. In a 3-day assay, MCF-10A/ErbB2 cells ablated for CD151 showed only a small and not significant decrease in colony size (Figure 5*B*, DMSO control). However, absence of CD151 sensitized tumor cell's response to inhibitors directed against ErbB2 (lapatinib), FAK (TAE-266), or MEK1/2 (U0126), causing a 46% to 51% decrease in colony size, compared with control cells. In contrast, CD151 ablation had little effect on tumor cell responsiveness to doxorubicin, a conventional chemotherapeutic agent (Figure 5*B*).

To recapitulate *in vivo* effects described in Figure 3*B*, we then analyzed CD151 effects on cell survival and proliferation. In a 5-day assay (Figure 5*C*, *a-c*) CD151 ablation markedly increased the percentage of

caspase 3–positive cells, but not Ki-67–positive cells. These changes were also accompanied by reduced nuclear translocation of ERK (Figure 5*C*, *e* and *f*), consistent with reduced ERK activation *in vivo* (Figure 4*A*) and *in vitro* (Figure 6*D*).

CD151-Mediated Tumor Progression Correlates with Cell Motility and Invasion

Given the impact of CD151 removal on spontaneous metastasis (Figure 2) and its functional link to EGFR [10], we tested whether CD151 collaborates with EGFR to accelerate early steps of metastasis involving tumor motility and invasiveness. As shown in Figure 6*A*, ablation of CD151 markedly decreased the random motility of MCF-10A/ErbB2 cells by 30% to 40% on stimulation by EGF, but not transforming growth factor β (TGF-β). In addition, removal of CD151 reduced transendothelial migration by 50% (Figure 6*B*). Furthermore, in the absence of CD151, EGF-stimulated invasion of MCF-10A/ErbB2 cells through Matrigel was significantly impaired (Figure 6*C*). Next, we tested whether CD151 impacts the signaling of EGFR or EGFR/ErbB2 heterodimers in MCF-10A/ErbB2 cells [43]. As anticipated, EGF-stimulated activation of FAK was markedly diminished in CD151-deficient cells (Figure 6*D*, *lanes 4-6*), compared with control cells (Figure 6*A*, *lanes 1-3*). Activation of ERK was also reduced, although not quite to the same extent as seen in mouse tumor samples (Figure 4*A*).

CD151 Mediates Mammary Tumorigenesis by Impacting Function and Signaling of Integrin $\alpha_6\beta_4$

Also, we examined the collaboration of CD151 with $\alpha_6\beta_4$ integrin, a major partner of CD151 in mammary epithelial cells [10,12]. By coimmunoprecipitation, a physical association of CD151 with α_6 and β_4 integrins was verified in mammary epithelial cells isolated from ErbB2-transgenic mice (Figure 7*A*). A crucial role of $\alpha_6\beta_4$ integrin is also supported by anti-$\alpha_6\beta_4$ antibody (GöH3) inhibition of acinar-like structures formed by MCF-10A/ErbB2 cells under three-dimensional culture (Figure 7*B*). This inhibition is even stronger than seen with anti-CD151 antibody (1A5) but similar to that elicited by CD151 removal (Figure 5*A*). To further demonstrate a functional link between CD151 and $\alpha_6\beta_4$, we performed CD151 mutant rescue experiments. Reexpression of CD151 (knockdown insensitive) in CD151 knockdown cells largely restored acinar-like structures (Figure 7*C*). In contrast, reconstitution with CD151 "EC mutant," which is defective in $\alpha_6\beta_4$ association [30], failed to rescue the effect of CD151 knockdown (Figure 7*C*).

Furthermore, we obtained evidence that CD151 regulates $\alpha_6\beta_4$ integrin phosphorylation at key sites involved in the transition from normal polarized epithelium to cell migration and invasion [27,28]. As shown in Figure 8*A*, tumors derived from CD151-null mice exhibited a marked reduction in β_4 integrin phosphorylation at the PKC-dependent S1424 residue [28] (*compare lanes 5-8 with 1-4*). A similar change was observed in β_4 S1356 phosphorylation (Figure 8*A*, *lanes 5-8*),
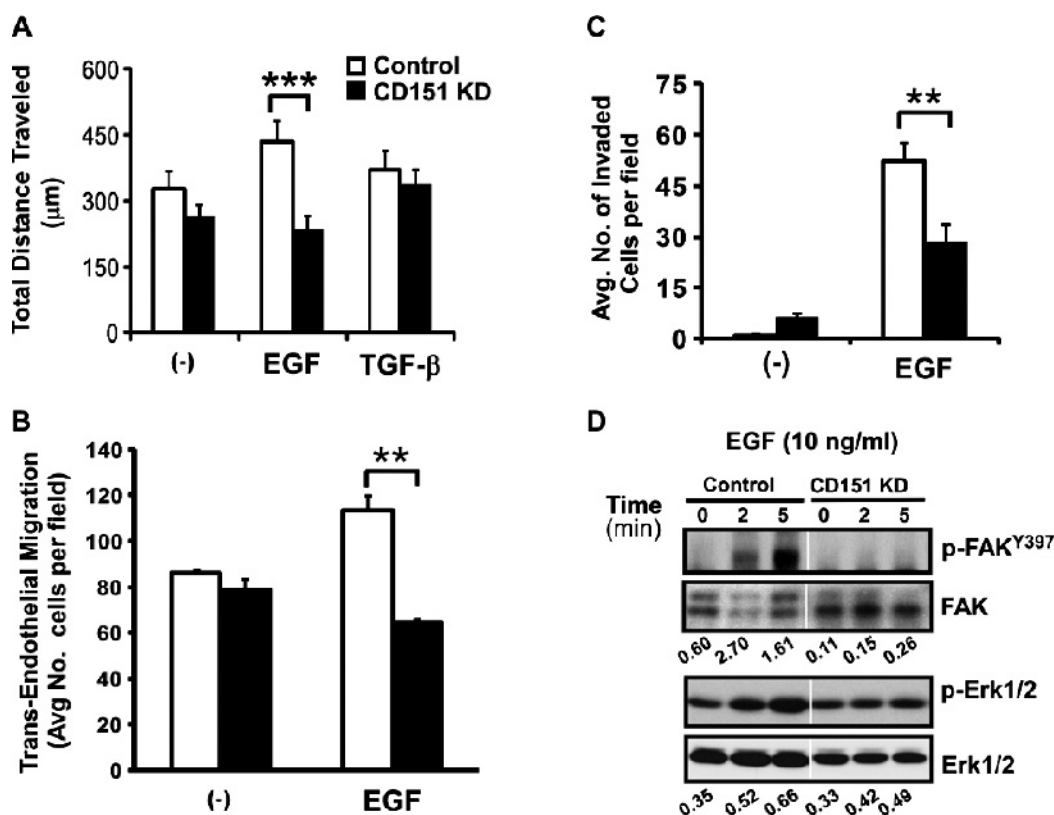
Figure 6. Ablation of CD151 inhibits tumor cell motility, invasion, and signaling. (A) To assess random motility, MCF-10A/ErbB2 cells (with or without CD151 knockdown) were treated with or without 10 ng/ml EGF or 5 ng/ml TGF-β1 for 12 hours. Twenty individual cells per treatment were tracked, and average distances traveled were calculated (mean ± SEM). (B) Differences in transendothelial migration (mean ± SEM, $n = 6$). EGF (10 ng/ml) was added to the bottom chamber as chemoattractant. (C) Invasive capabilities of MCF-10A/ErbB2 cells ± CD151 ablation (mean ± SEM, $n = 3$) and ±10 ng/ml EGF stimulation. **$P < .01$, ***$P < .001$. (D) Activation of FAK and ERK in response to EGF stimulation. The ratios of phosphorylated *versus* total proteins were calculated by densitometry analyses.
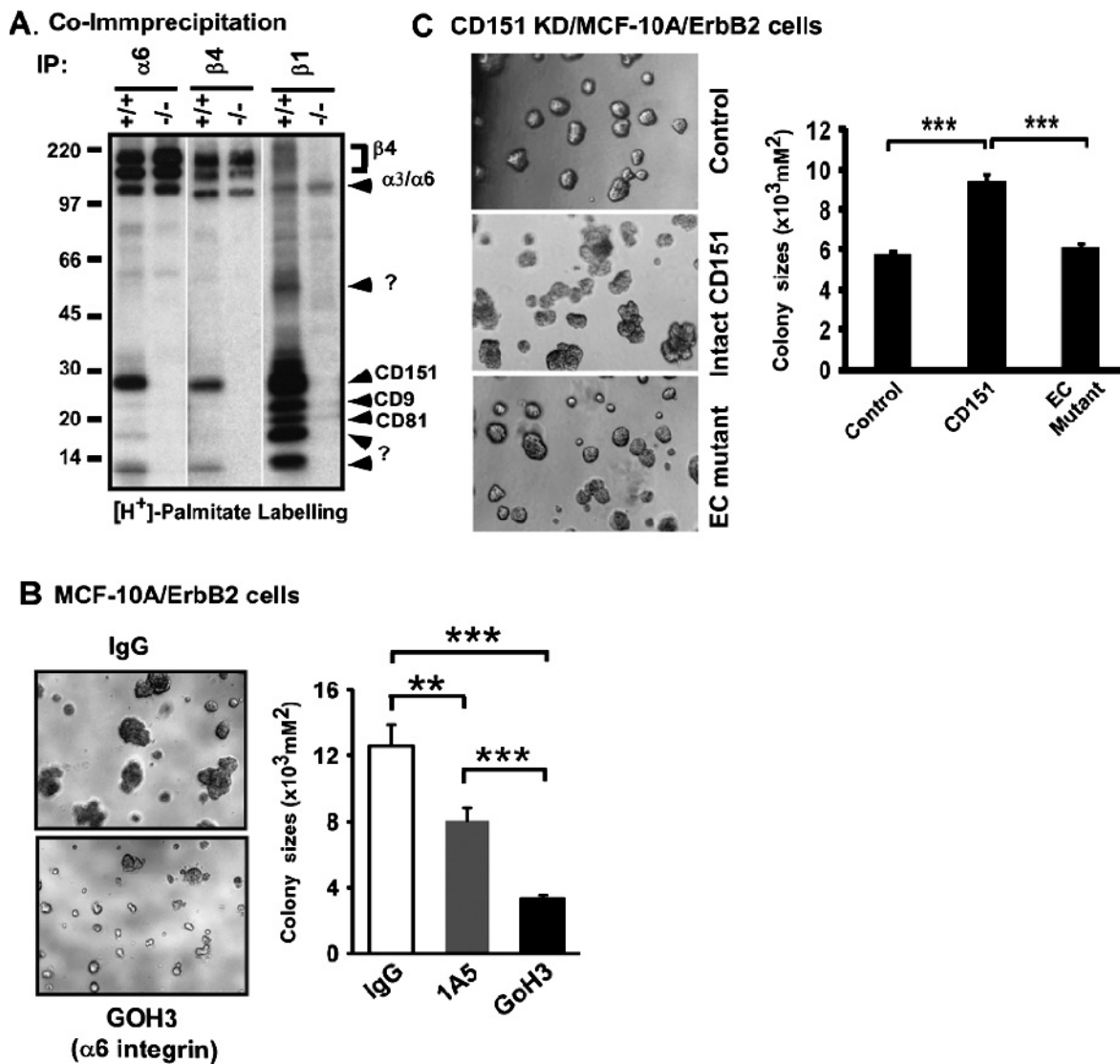
Figure 7. CD151-mediated tumorigenesis involves $\alpha_6\beta_4$ integrin. (A) Mouse stable cell lines were established from primary mouse ErbB2 tumors, labeled with [^{3}H]-palmitate and immunoprecipitated with integrin-specific monoclonal antibodies as described [10,29]. (B) Human MCF-10A/ErbB2 cells were treated with nonimmune IgG or GöH3 (anti–integrin α_6) or 1A5 (anti–CD151) antibodies for 5 days and photographed. Mean sizes of colonies are indicated. (C) Human MCF-10A/ErbB2 cells were infected with virus expressing intact human CD151 or EC mutant (defective in $\alpha_6\beta_4$ integrin association) as previously described [30]. The EC mutant was generated by replacing a stretch of amino acids located in the large extracellular loop of CD151 protein with a corresponding portion from the non–integrin-binding tetraspanin CD231/A15.

which is mediated by PKC and/or ERK1/2 [27]. To confirm these differences, we evaluated β_4 integrin phosphorylation in MCF-10A/ErbB2 cells. Again, CD151 ablation caused a reduction in constitutive β_4 integrin phosphorylation at S1424 (Figure 8B). Constitutive β_4 S1356 phosphorylation was not diminished, perhaps because it was already low. On EGF stimulation, β_4 integrin phosphorylation at both S1424 and S1356 sites was reduced when CD151 was absent.

CD151 Gene Expression Correlates with ErbB2-Positive Breast Cancer Patient Survival

Having seen a strong *in vivo* effect of CD151 deletion on tumor appearance and metastasis (Figures 1 and 2), we then investigated CD151 expression with respect to ErbB2$^+$ breast cancer patient survival. In a gene expression data set of 132 human primary tumor samples [44], the concomitant expression of *CD151* and *ErbB2* genes is strongly predictive of metastasis-free survival (P = .0082; Figure 9A). Notably, for patients with a good prognosis, 5-year metastasis-free survival exceeded 50%, whereas those with a poor prognosis showed only 10% survival. In another independent breast tumor data set of 295 human samples [45], elevated expression of both *CD151* and *ErbB2* genes was again predictive of metastasis-free survival (P = .047; Figure 9A, *right panel*). However, in neither data set was expression of either *CD151* or *ErbB2* genes alone associated with metastasis-free survival (P > .05 in all four cases).

Discussion

With combined approaches of an animal genetic model and a three-dimensional cell culture model, backed up by human patient survival data, we demonstrate that tetraspanin CD151 is a critical regulator of

ErbB2 oncogene–evoked mammary tumorigenesis. Deletion of CD151 markedly impaired mammary tumor onset, decreased tumor cell survival, and decreased spontaneous metastasis in ErbB2-transgenic mice. In three-dimensional cultured cells, CD151 removal again decreased mammary epithelial cell survival while also decreasing cell motility and invasion. Functional consequences of CD151 absence, in both the mouse model and in three-dimensional cell culture, were accompanied by substantial decreases in the activation of ERK and FAK and in the phosphorylation of β_4 integrin by PKC and ERK. Events affected elsewhere in mammary tumor cells by CD151 or LB integrins (e.g., primary tumor growth rate [10,46], TGF-β signaling [8], AKT activation [47], and STAT3 activation [42]) were not altered in our ErbB2-driven mammary cells, either in mouse tumors and/or in three-dimensional culture. Our novel findings lead to the working model outlined in Figure 9C.

CD151 Accelerates the Onset of ErbB2-Driven Mammary Tumors

Our analyses using ErbB2 transgenic mice provide the first demonstration that CD151 promotes mammary tumor initiation. Delayed tumor onset on CD151 deletion (70-100 days) is substantially greater than the 35-day delay caused by β_4 cytoplasmic tail truncation [42].
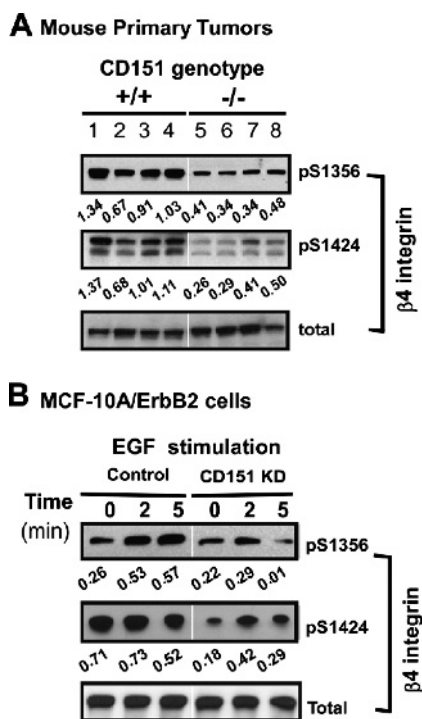
Figure 8. Impact of CD151 removal on $\alpha_6\beta_4$ integrin phosphorylation. (A) Tissue extracts prepared from four representative tumors from CD151 +/+ and −/− mice were blotted with the indicated antibodies to show β_4 integrin phosphorylation. (B) Phosphorylation of β_4 integrin in cultured MCF-10A/ErB2 cells was analyzed. Control shRNA- and CD151 shRNA-expressing cells were stimulated with EGF (10 ng/ml) for indicated times (minutes) and lysed in RIPA buffer. Antibodies used to assess phosphorylation of β_4 integrin were described [27,28]. Numbers under blots indicate phosphorylated/total protein ratios from densitometry analyses. All samples were run on the same gels and blotted simultaneously with the same nitrocellulose membranes.

This longer delay may be at least partly due to CD151 differentially affecting contributions of multiple integrins ($\alpha_3\beta_1$, $\alpha_6\beta_1$, and $\alpha_6\beta_4$). We suspect that CD151 acts by modulating LB integrins and other proteins in tetraspanin-enriched microdomains (TEMs). In this regard, CD151 can affect diffusion mode [15], distribution [10], membrane turnover [48], and glycosylation [49] of LB integrins. Of particular relevance to tumor onset, CD151 may affect α_6 integrins, which can regulate functions of mammary epithelial stem and progenitor cells, both of which are also essential targets of the *ErbB2* oncogene [50,51]. Unexpectedly, mice lacking one or both copies of CD151 showed comparably delayed tumor onset and comparably reduced tumor metastasis. We speculate that removing one CD151 allele might impair protumor contributions of $\alpha_6\beta_4$, without much affecting $\alpha_3\beta_1$. By contrast, on removing both alleles of CD151, additional loss of protumor $\alpha_6\beta_4$ effects might be counterbalanced by the partial loss of suppressor effects of $\alpha_3\beta_1$.

CD151 ablation did not much affect ErbB2 and EGFR activation but did diminish their functions (i.e., responses to EGF, signaling through FAK and ERK, and conventional PKC [cPKC]– and ERK-dependent phosphorylations of β_4). Notably, FAK has itself been linked to breast cancer initiation [52,53]. Increased MCF-10A/ErbB2 cell sensitivity to drugs targeting FAK, ErbB2/EGFR, and MEK/ERK is consistent with these signaling pathways being weakened, as a consequence of CD151 removal.

Analysis of mammary gland architecture revealed a mild defect in secondary branching, which could influence tumor formation. However, normal mammary gland development is similarly altered by CD151 deletion even when the *ErbB2* transgene is absent. Further studies are needed to clarify the mechanistic details underlying CD151 effects on mammary gland development and ErbB2-driven tumorigenesis.

CD151-Mediated Tumorigenesis Correlates with Survival rather than Proliferation

The impact of CD151 removal on ErbB2-evoked mammary tumor onset may be due to diminished survival, rather than diminished cell proliferation, as seen in both tumor cells and in MCF-10A/ErbB2 model cells. Caspase 3-staining showed ∼6% more cell death occurring in knockout cells, giving a 1.06-fold advantage to wild-type cells. During the three generations (followed for 3 weeks as in Figure 1B), an increased growth rate is not that obvious ($1.06^3 = 1.19$). However, during the ∼25 generations needed for single initiated cells to grow into visible tumors ($1.06^{25} = 4.3$), a substantial difference in tumor size is predicted (about four-fold), which would be consistent with a delay in appearance of knockout tumors.

Typically, ErbB2 signals through the RAS/RAF/MEK/ERK pathway to stimulate cell proliferation and migration, whereas it uses the PI3K/AKT pathway for survival [54]. By contrast, our results show CD151 supporting ERK activation, not to affect proliferation but rather to influence survival in an AKT-independent manner. Although our results are perhaps atypical, at least one other study has linked ErbB2-dependent activation of ERK1/2 to cell survival [55], and ERK may promote AKT-independent survival by inactivating the proapoptotic BAD protein [56]. Our results also show CD151-dependent activation of FAK in association with cell survival, consistent with other studies linking FAK to cell survival [57]. Also, CD151 may use the NF-κB pathway to mediate mammary cell survival. In this regard, forced expression of NF-κB protein p65/RelA in CD151-deficient
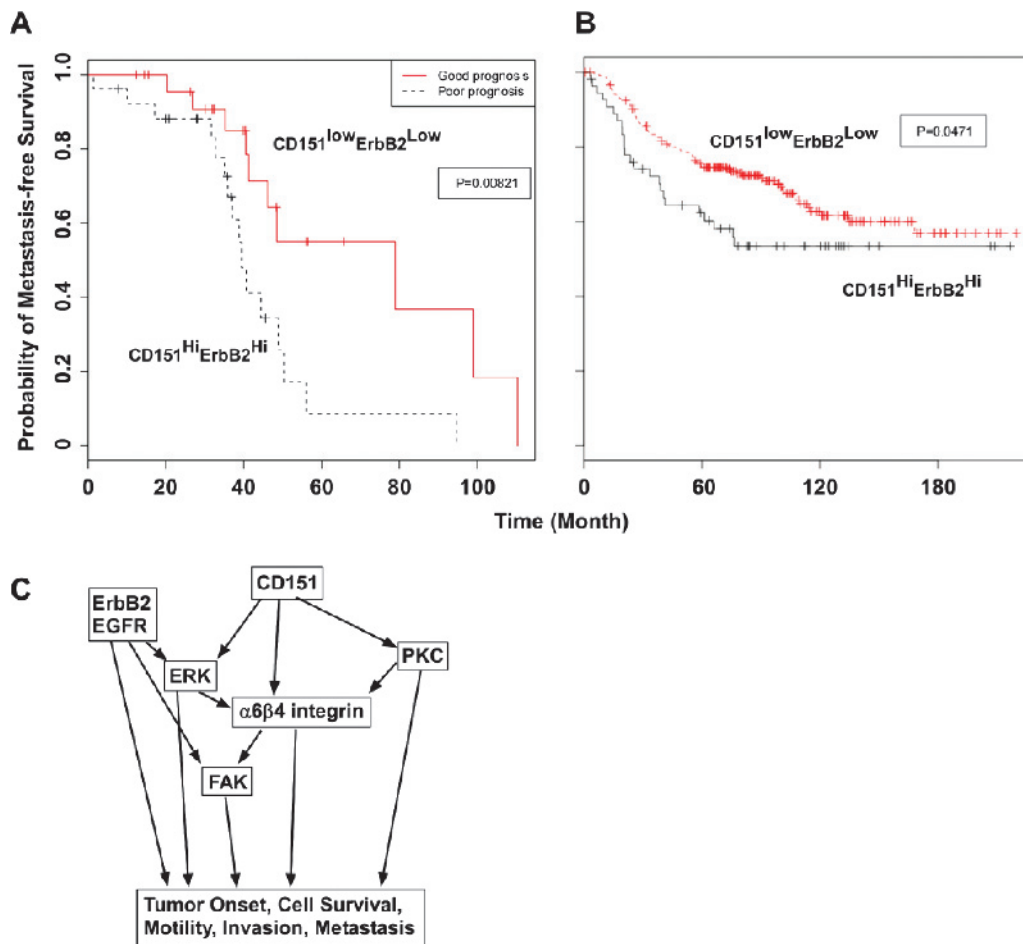
Figure 9. Correlation of CD151 gene expression with metastasis-free survival of breast cancer patients. (A) Kaplan-Meier metastasis-free survival curves were constructed from data sets containing CD151 and ErbB2 gene expression information from 132 human primary tumor samples [44]. (B) Similar curves are constructed from data sets containing CD151 and ErbB2 information from 295 human samples [45]. Statistical significance (in A and B) is evaluated using the log-rank test. (C) A working model is shown for CD151 function during ErbB2-evoked mammary tumor onset and metastasis.

MCF-10A/ErbB2 cells markedly decreased caspase 3–positive cells in acinar-like structures (not shown).

CD151 Facilitates Spontaneous Mammary Tumor Metastasis

In various tumor cell injection models, CD151 sometimes supported *in vitro* cell invasion or experimental metastasis (Introduction), but its role in spontaneous metastasis was not addressed. Here we show that CD151 deletion caused a significant reduction in spontaneous metastases in MMTV-ErbB2 mice. In both primary and metastatic samples, CD151 loss yielded a transition from irregular invasive-like borders to smoother sheet-like epithelial morphologies, with a marked reduction in recruitment of stromal-like cells. These changes suggest altered tumor cell interactions with local microenvironment—a topic that requires further study.

CD151 ablation from ErbB2$^+$ cells caused marked reductions in tumor cell invasion, random migration, and transendothelial migration, consistent with decreased metastatic capability. CD151 may drive tumor metastasis largely through EGFR-, FAK-, and PKC-mediated pathways. A close CD151 connection to FAK activation (in both tumors and in MCF-10A/ErbB2 cells) is consistent with CD151 and FAK effects on breast cancer cell sensitivity to ErbB2 antagonists [12]. cPKC isoforms (i.e., PKCα) are crucial for $\alpha_6\beta_4$ and ErbB recep-

tor function during cell migration and metastasis [28,58]. Also, cPKC (together with ERK) supports phosphorylation of β_4 at S1356 and S1424 [27,28]. Reduced phosphorylation at these sites in CD151-deficient cells is consistent not only with dysregulated cPKC function but also with diminished cell migration and invasion [27]. Diminished FAK activation was not accompanied by diminished Src and p130Cas activation, thus indicating a more restricted signaling phenotype in our ErbB2-driven mammary tumors, compared with CD151-ablated lung adenocarcinoma cells [59]. As suggested [10], Lck may possibly replace Src in the FAK signaling pathway.

CD151 can associate and functionally collaborate not only with $\alpha_6\beta_4$ but also with $\alpha_3\beta_1$, as seen in ErbB2$^+$ breast cancer cell lines [12]. Consistent with this, the absence of CD151 affected cell adhesion to laminin 5 (ligand for $\alpha_3\beta_1$ and $\alpha_6\beta_4$). In other breast cancer cell lines (not expressing ErbB2), integrin $\alpha_3\beta_1$ can contribute to *in vitro* invasion and *in vivo* experimental metastasis (Figure W4) [60,61]. However, we suspect that, for ErbB2$^+$ breast cancer, CD151 is mostly supporting functions of $\alpha_6\beta_4$ and perhaps also of $\alpha_6\beta_1$. In this regard, MCF-10A/ErbB2 cell colony formation largely involved CD151 collaboration with α_6 integrins (e.g., Figure 7), whereas inhibition of $\alpha_3\beta_1$ minimally affected the size of colonies formed by three-dimensional cultured mammary cells (not shown). Nonetheless, we have not ruled out a role for

$\alpha_3\beta_1$ in CD151-dependent regulation of ErbB2-driven tumor onset and metastasis *in vivo*.

Where Is CD151 Functioning?

Results from our three-dimensional cell culture analyses of human mammary epithelial cells largely recapitulate the *in vivo* impact of CD151 removal, confirming a direct role of CD151 in ErbB2-evoked mammary tumorigenesis and metastasis. Nonetheless, CD151 could also affect ErbB2$^+$ tumor onset and metastasis indirectly through other cells and tissues, such as endothelial cells [20], kidneys [23,24,62], or immune cells [63]. Although tumor angiogenesis did not seem to be diminished at primary tumor sites, we cannot rule out CD151 contributing to metastasis by supporting lung endothelial cell function [64]. Although CD151 deletion can seriously impact kidney function in FVB mice [24], we avoided this problem by backcrossing CD151-null mice into FVB for only three generations. Indeed, our results strongly suggest that the effects of CD151 on tumor onset and metastasis are independent of kidney pathology. With respect to potential immune cell contributions, CD151 deletion from tumor-bearing mice so far does not affect immune cell subset sizes, activation, trafficking, or infiltration into tumors [64].

CD151 as a Promising Therapeutic Target

Our results consistently demonstrate that CD151 supports mammary tumorigenesis, particularly with respect to tumor onset, metastasis, and survival, in association with key signaling pathways involving FAK, ERK, and integrin β_4 phosphorylation. Given the strong correlation between CD151 expression and poor metastasis-free survival of ErbB2$^+$ breast cancer patients (Figure 9, *A* and *B*) and the role of CD151 in basal-like breast tumor malignancy [10,11,46], we predict that targeting CD151 could serve as another treatment option for breast cancer patients with ER$^-$ tumors. It remains to be seen whether targeting of CD151 would have adverse effects in the skin and kidney [23,24,62] or would have minimal effects on the skin or kidney or any other normal cells and tissues *in vivo* [65].

References

[1] Lohrisch C and Piccart M (2001). An overview of HER2. *Semin Oncol* **28**, 3–11.

[2] Eccles SA (2001). The role of c-erbB-2/HER2/neu in breast cancer progression and metastasis. *J Mammary Gland Biol Neoplasia* **6**, 393–406.

[3] Esteva FJ, Cheli CD, Fritsche H, Fornier M, Slamon D, Thiel RP, Luftner D, and Ghani F (2005). Clinical utility of serum HER2/neu in monitoring and prediction of progression-free survival in metastatic breast cancer patients treated with trastuzumab-based therapies. *Breast Cancer Res* **7**, R436–R443.

[4] Esteva FJ, Valero V, Booser D, Guerra LT, Murray JL, Pusztai L, Cristofanilli M, Arun B, Esmaeli B, Fritsche HA, et al. (2002). Phase II study of weekly docetaxel and trastuzumab for patients with HER-2–overexpressing metastatic breast cancer. *J Clin Oncol* **20**, 1800–1808.

[5] Hemler ME (2001). Specific tetraspanin functions. *J Cell Biol* **155**, 1103–1107.

[6] Hemler ME (2008). Targeting of tetraspanin proteins—potential benefits and strategies. *Nat Rev Drug Discov* **7**, 747–758.

[7] Stipp CS (2010). Laminin-binding integrins and their tetraspanin partners as potential antimetastatic targets. *Expert Rev Mol Med* **12**, e3.

[8] Sadej R, Romanska H, Kavanagh D, Baldwin G, Takahashi T, Kalia N, and Berditchevski F (2010). Tetraspanin CD151 regulates transforming growth factor β signaling: implication in tumor metastasis. *Cancer Res* **70**, 6059–6070.

[9] Romanska HM and Berditchevski F (2011). Tetraspanins in human epithelial malignancies. *J Pathol* **223**, 4–14.

[10] Yang XH, Richardson AL, Torres-Arzayus MI, Zhou P, Sharma C, Kazarov AR, Andzelm MM, Strominger JL, Brown M, and Hemler ME (2008). CD151 accelerates breast cancer by regulating α_6 integrin function, signaling, and molecular organization. *Cancer Res* **68**, 3204–3213.

[11] Kwon MJ, Park S, Choi JY, Oh E, Kim YJ, Park YH, Cho EY, Nam SJ, Im YH, Shin YK, et al. (2012). Clinical significance of CD151 overexpression in subtypes of invasive breast cancer. *Br J Cancer* **106**, 923–930.

[12] Yang XH, Flores LM, Li Q, Zhou P, Xu F, Krop IE, and Hemler ME (2010). Disruption of laminin-integrin-CD151–focal adhesion kinase axis sensitizes breast cancer cells to ErbB2 antagonists. *Cancer Res* **70**, 2256–2263.

[13] Hemler ME (2005). Tetraspanin functions and associated microdomains. *Nat Rev Mol Cell Biol* **6**, 801–811.

[14] Sterk LM, Geuijen CA, van den Berg JG, Claessen N, Weening JJ, and Sonnenberg A (2002). Association of the tetraspanin CD151 with the laminin-binding integrins $\alpha_3\beta_1$, $\alpha_6\beta_1$, $\alpha_6\beta_4$ and $\alpha_7\beta_1$ in cells in culture and *in vivo*. *J Cell Sci* **115**, 1161–1173.

[15] Yang XH, Mirchev R, Deng X, Yacono P, Yang HL, Golan DE, and Hemler ME (2012). CD151 restricts α_6 integrin diffusion mode. *J Cell Sci* **125**, 1478–1487.

[16] Owens DM and Watt FM (2001). Influence of β1 integrins on epidermal squamous cell carcinoma formation in a transgenic mouse model: $\alpha_3\beta_1$, but not $\alpha_2\beta_1$, suppresses malignant conversion. *Cancer Res* **61**, 5248–5254.

[17] Owens DM, Romero MR, Gardner C, and Watt FM (2003). Suprabasal $\alpha_6\beta_4$ integrin expression in epidermis results in enhanced tumourigenesis and disruption of TGFβ signalling. *J Cell Sci* **116**, 3783–3791.

[18] Dajee M, Lazarov M, Zhang JY, Cai T, Green CL, Russell AJ, Marinkovich MP, Tao S, Lin Q, Kubo Y, et al. (2003). NF-κB blockade and oncogenic Ras trigger invasive human epidermal neoplasia. *Nature* **421**, 639–643.

[19] Margadant C, Raymond K, Kreft M, Sachs N, Janssen H, and Sonnenberg A (2009). Integrin $\alpha_3\beta_1$ inhibits directional migration and wound re-epithelialization in the skin. *J Cell Sci* **122**, 278–288.

[20] Takeda Y, Kazarov AR, Butterfield CE, Hopkins BD, Benjamin LE, Kaipainen A, and Hemler ME (2007). Deletion of tetraspanin Cd151 results in decreased pathologic angiogenesis *in vivo* and *in vitro*. *Blood* **109**, 1524–1532.

[21] Ursini-Siegel J, Schade B, Cardiff RD, and Muller WJ (2007). Insights from transgenic mouse models of ERBB2-induced breast cancer. *Nat Rev Cancer* **7**, 389–397.

[22] Guy CT, Webster MA, Schaller M, Parsons TJ, Cardiff RD, and Muller WJ (1992). Expression of the *neu* protooncogene in the mammary epithelium of transgenic mice induces metastatic disease. *Proc Natl Acad Sci USA* **89**, 10578–10582.

[23] Sachs N, Kreft M, van den Bergh Weerman MA, Beynon AJ, Peters TA, Weening JJ, and Sonnenberg A (2006). Kidney failure in mice lacking the tetraspanin CD151. *J Cell Biol* **175**, 33–39.

[24] Baleato RM, Guthrie PL, Gubler MC, Ashman LK, and Roselli S (2008). Deletion of Cd151 results in a strain-dependent glomerular disease due to severe alterations of the glomerular basement membrane. *Am J Pathol* **173**, 927–937.

[25] Torres-Arzayus MI, Font de Mora J, Yuan J, Vazquez F, Bronson R, Rue M, Sellers WR, and Brown M (2004). High tumor incidence and activation of the PI3K/AKT pathway in transgenic mice define AIB1 as an oncogene. *Cancer Cell* **6**, 263–274.

[26] Debnath J and Brugge JS (2005). Modelling glandular epithelial cancers in three-dimensional cultures. *Nat Rev Cancer* **5**, 675–688.

[27] Frijns E, Sachs N, Kreft M, Wilhelmsen K, and Sonnenberg A (2010). EGF-induced MAPK signaling inhibits hemidesmosome formation through phosphorylation of the integrin β4. *J Biol Chem* **285**, 37650–37662.

[28] Germain EC, Santos TM, and Rabinovitz I (2009). Phosphorylation of a novel site on the β4 integrin at the trailing edge of migrating cells promotes hemidesmosome disassembly. *Mol Biol Cell* **20**, 56–67.

[29] Yang X, Kovalenko OV, Tang W, Claas C, Stipp CS, and Hemler ME (2004). Palmitoylation supports assembly and function of integrin-tetraspanin complexes. *J Cell Biol* **167**, 1231–1240.

[30] Zevian S, Winterwood NE, and Stipp CS (2010). Structure-function analysis of tetraspanin CD151 reveals distinct requirements for tumor cell behaviors mediated by $\alpha_3\beta_1$ *versus* $\alpha_6\beta_4$ integrin. *J Biol Chem* **286**, 7496–7506.

[31] Yang XW, Claas C, Kraeft SK, Chen LB, Wang ZM, Kreidberg JA, and Hemler ME (2002). Palmitoylation of tetraspanin proteins: modulation of CD151 lateral interactions, subcellular distribution, and integrin-dependent cell morphology. *Mol Biol Cell* **13**, 767–781.

[32] Lukes L, Crawford NP, Walker R, and Hunter KW (2009). The origins of breast cancer prognostic gene expression profiles. *Cancer Res* **69**, 310–318.

[33] Rosner A, Miyoshi K, Landesman-Bollag E, Xu X, Seldin DC, Moser AR, MacLeod CL, Shyamala G, Gillgrass AE, and Cardiff RD (2002). Histological differences between ErbB/Ras and wnt pathway transgenic mammary tumors. *Am J Pathol* **161**, 1087–1097.

[34] Chatterjee G, Rosner A, Han Y, Zelazny ET, Li BL, Cardiff RD, and Perkins AS (2002). Acceleration of mouse mammary tumor virus–induced murine mammary tumorigenesis by a p53(172H) transgene—influence of FVB background identification of novel sites of on tumor latency and proviral insertion. *Am J Pathol* **161**, 2241–2253.

[35] Carriere A, Cargnello M, Julien LA, Gao H, Bonneil E, Thibault P, and Roux PP (2008). Oncogenic MAPK signaling stimulates mTORC1 activity by promoting RSK-mediated raptor phosphorylation. *Curr Biol* **18**, 1269–1277.

[36] Carriere A, Ray H, Blenis J, and Roux PP (2008). The RSK factors of activating the Ras/MAPK signaling cascade. *Front Biosci* **13**, 4258–4275.

[37] Hynes NE and Watson CJ (2010). Mammary gland growth factors: roles in normal development and in cancer. *Cold Spring Harb Perspect Biol* **2**, a003186.

[38] Pontier SM and Muller WJ (2009). Integrins in mammary-stem-cell biology and breast-cancer progression—a role in cancer stem cells? *J Cell Sci* **122**, 207–214.

[39] Wiseman BS and Werb Z (2002). Stromal effects on mammary gland development and breast cancer. *Science* **296**, 1046–1049.

[40] Muthuswamy SK, Li D, Lelievre S, Bissell MJ, and Brugge JS (2001). ErbB2, but not ErbB1, reinitiates proliferation and induces luminal repopulation in epithelial acini. *Nat Cell Biol* **3**, 785–792.

[41] Brantley-Sieders DM, Zhuang G, Hicks D, Bin Fang W, Hwang Y, Cates JMM, Coffman K, Jackson D, Bruckheirner E, Muraoka-Cook RS, et al. (2008). The receptor tyrosine kinase EphA2 promotes mammary adenocarcinoma tumorigenesis and metastatic progression in mice by amplifying ErbB2 signaling. *J Clin Invest* **118**, 64–78.

[42] Guo W, Pylayeva Y, Pepe A, Yoshioka T, Muller WJ, Inghirami G, and Giancotti FG (2006). β_4 integrin amplifies ErbB2 signaling to promote mammary tumorigenesis. *Cell* **126**, 489–502.

[43] DeFazio-Eli L, Strommen K, Dao-Pick T, Parry G, Goodman L, and Winslow J (2011). Quantitative assays for the measurement of HER1-HER2 heterodimerization and phosphorylation in cell lines and breast tumors: applications for diagnostics and targeted drug mechanism of action. *Breast Cancer Res* **13**, R44.

[44] Chanrion M, Negre V, Fontaine H, Salvetat N, Bibeau F, Mac Grogan G, Mauriac L, Katsaros D, Molina F, Theillet C, et al. (2008). A gene expression signature that can predict the recurrence of tamoxifen-treated primary breast cancer. *Clin Cancer Res* **14**, 1744–1752.

[45] van de Vijver MJ, He YD, van't Veer LJ, Dai H, Hart AA, Voskuil DW, Schreiber GJ, Peterse JL, Roberts C, Marton MJ, et al. (2002). A gene-expression signature as a predictor of survival in breast cancer. *N Engl J Med* **347**, 1999–2009.

[46] Sadej R, Romanska H, Baldwin G, Gkirtzimanaki K, Novitskaya V, Filer AD, Krcova Z, Kusinska R, Ehrmann J, Buckley CD, et al. (2009). CD151 regulates tumorigenesis by modulating the communication between tumor cells and endothelium. *Mol Cancer Res* **7**, 787–798.

[47] Novitskaya V, Romanska H, Dawoud M, Jones JL, and Berditchevski F (2010). Tetraspanin CD151 regulates growth of mammary epithelial cells in three-dimensional extracellular matrix: implication for mammary ductal carcinoma in situ. *Cancer Res* **70**, 4698–4708.

[48] Winterwood NE, Varzavand A, Meland MN, Ashman LK, and Stipp CS (2006). A critical role for tetraspanin CD151 in $\alpha_3\beta_1$ and $\alpha_6\beta_4$ integrin-dependent tumor cell functions on laminin-5. *Mol Biol Cell* **17**, 2707–2721.

[49] Baldwin G, Novitskaya V, Sadej R, Pochec E, Litynska A, Hartmann C, Williams J, Ashman L, Eble JA, and Berditchevski F (2008). Tetraspanin CD151 regulates glycosylation of $\alpha_3\beta_1$ integrin. *J Biol Chem* **283**, 35445–35454.

[50] Jeselsohn R, Brown NE, Arendt L, Klebba I, Hu MG, Kuperwasser C, and Hinds PW (2010). Cyclin D1 kinase activity is required for the self-renewal of mammary stem and progenitor cells that are targets of MMTV-ErbB2 tumorigenesis. *Cancer Cell* **17**, 65–76.

[51] Stingl J, Eirew P, Ricketson I, Shackleton M, Vaillant F, Choi D, Li HI, and Eaves CJ (2006). Purification and unique properties of mammary epithelial stem cells. *Nature* **439**, 993–997.

[52] Luo J, Yin X, Ma T, and Lu J (2010). Stem cells in normal mammary gland and breast cancer. *Am J Med Sci* **339**, 366–370.

[53] Lahlou H, Sanguin-Gendreau V, Frame MC, and Muller WJ (2012). Focal adhesion kinase contributes to proliferative potential of ErbB2 mammary tumour cells but is dispensable for ErbB2 mammary tumour induction in vivo. *Breast Cancer Res* **14**, R36.

[54] Arias-Romero LE, Villamar-Cruz O, Pacheco A, Kosoff R, Huang M, Muthuswamy SK, and Chernoff J (2010). A Rac-Pak signaling pathway is essential for ErbB2-mediated transformation of human breast epithelial cancer cells. *Oncogene* **29**, 5839–5849.

[55] Haenssen KK, Caldwell SA, Shahriari KS, Jackson SR, Whelan KA, Klein-Szanto AJ, and Reginato MJ (2010). ErbB2 requires integrin α_5 for anoikis resistance via Src regulation of receptor activity in human mammary epithelial cells. *J Cell Sci* **123**, 1373–1382.

[56] Hartel FV, Holl M, Arshad M, Aslam M, Gunduz D, Weyand M, Micoogullari M, Abdallah Y, Piper HM, and Noll T (2010). Transient hypoxia induces ERK-dependent anti-apoptotic cell survival in endothelial cells. *Am J Physiol Cell Physiol* **298**, C1501–C1509.

[57] Luo M and Guan JL (2010). Focal adhesion kinase: a prominent determinant in breast cancer initiation, progression and metastasis. *Cancer Lett* **289**, 127–139.

[58] Kim J, Thorne SH, Sun L, Huang B, and Mochly-Rosen D (2011). Sustained inhibition of PKCα reduces intravasation and lung seeding during mammary tumor metastasis in an in vivo mouse model. *Oncogene* **30**, 323–333.

[59] Yamada M, Sumida Y, Fujibayashi A, Fukaguchi K, Sanzen N, Nishiuchi R, and Sekiguchi K (2008). The tetraspanin CD151 regulates cell morphology and intracellular signaling on laminin-511. *FEBS J* **275**, 3335–3351.

[60] Wang H, Fu W, Im JH, Zhou Z, Santoro SA, Iyer V, DiPersio CM, Yu QC, Quaranta V, Al-Mehdi A, et al. (2004). Tumor cell $\alpha_3\beta_1$ integrin and vascular laminin-5 mediate pulmonary arrest and metastasis. *J Cell Biol* **164**, 935–941.

[61] Mitchell K, Svenson KB, Longmate WM, Gkirtzimanaki K, Sadej R, Wang X, Zhao J, Eliopoulos AG, Berditchevski F, and Dipersio CM (2010). Suppression of integrin $\alpha_3\beta_1$ in breast cancer cells reduces cyclooxygenase-2 gene expression and inhibits tumorigenesis, invasion, and cross-talk to endothelial cells. *Cancer Res* **70**, 6359–6367.

[62] Crew VK, Burton N, Kagan A, Green CA, Levene C, Flinter F, Brady RL, Daniels G, and Anstee DJ (2004). CD 151, the first member of the tetraspanin (TM4) superfamily detected on erythrocytes, is essential for the correct assembly of human basement membranes in kidney and skin. *Blood* **104**, 2217–2223.

[63] Sheng KC, van Spriel AB, Gartlan KH, Sofi M, Apostolopoulos V, Ashman L, and Wright MD (2009). Tetraspanins CD37 and CD151 differentially regulate Ag presentation and T-cell co-stimulation by DC. *Eur J Immunol* **39**, 50–55.

[64] Takeda Y, Li Q, Kazarov AR, Epardaud M, Elpek K, Turley SJ, and Hemler ME (2011). Diminished metastasis in tetraspanin CD151-knockout mice. *Blood* **118**, 464–472.

[65] Wright MD, Geary SM, Fitter S, Moseley GW, Lau LM, Sheng KC, Apostolopoulos V, Stanley EG, Jackson DE, and Ashman LK (2004). Characterization of mice lacking the tetraspanin superfamily member CD151. *Mol Cell Biol* **24**, 5978–5988.
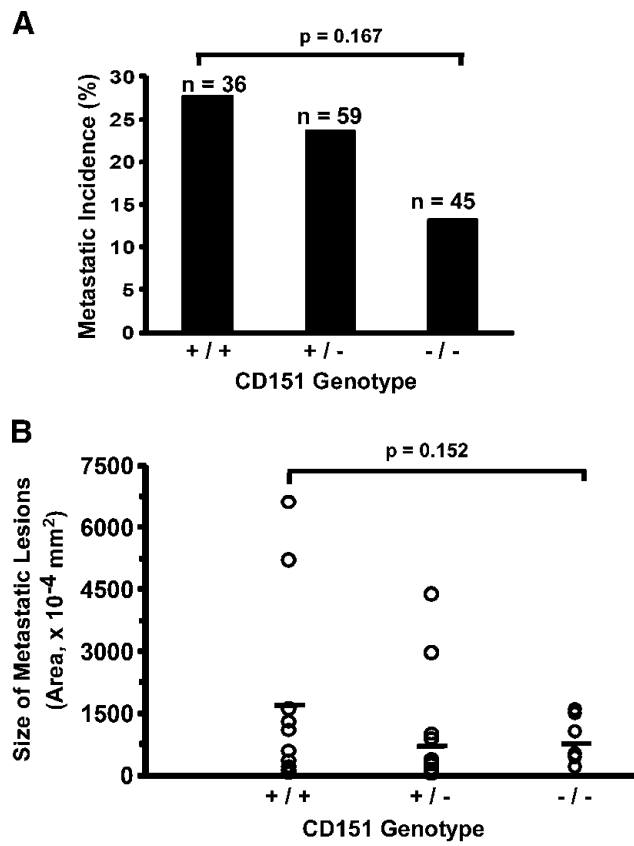
Figure W1. Effect of CD151 on mammary tumor metastasis. (A) Incidence of spontaneous pulmonary metastatic lesions in ErbB2 transgenic mice is indicated. (B) Effects of CD151 deletion on sizes of metastatic lesions (and mean size values) are shown.
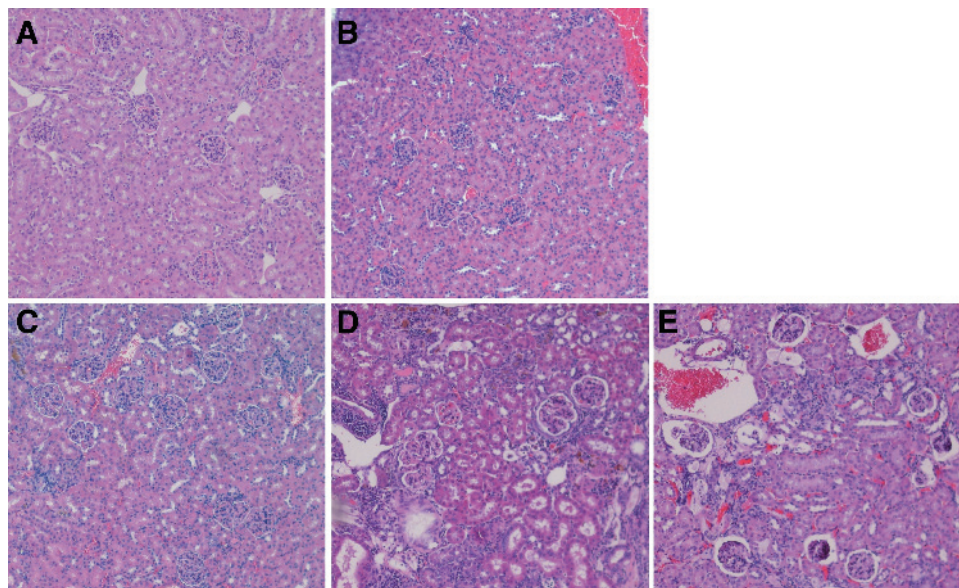
Figure W2. Hematoxylin and eosin staining of kidney sections from mice used in Figure 1*A*. At the end of *in vivo* tumor monitoring, kidneys were removed from (A) wild-type mice ($n = 6$), (B) CD151$^{+/-}$ mice ($n = 4$), (C-E) CD151 KO mice ($n = 11$): C, mild; D, intermediate; E, severe.
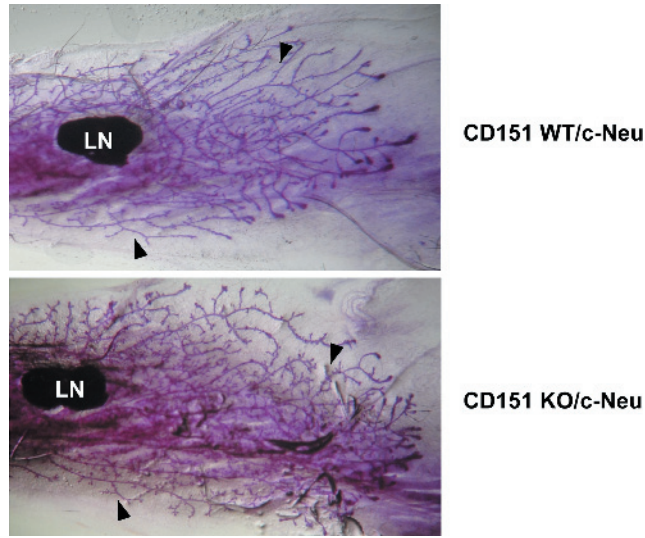
Figure W3. Effect of CD151 removal on outgrowth of mammary glands in ErbB2-transgenic mice. Representative whole-mounted mammary glands from 6- to 8-week-old ErbB2-positive mice ($n = 3$). Results are representative of three mice per group.
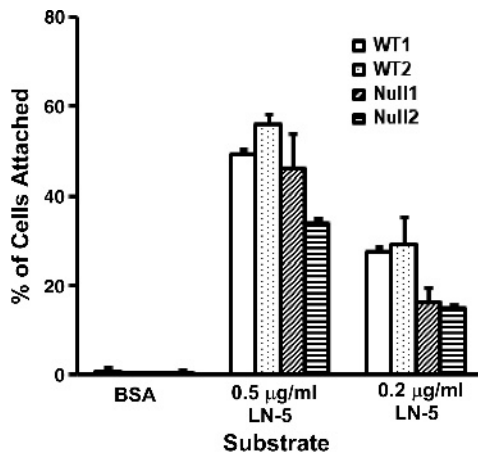
Figure W4. Absence of CD151 affects tumor cell adhesion. Cell lines were derived from tumors developed in CD151 WT and KO mice and then analyzed for adhesion to laminin 5–coated plastic surfaces at different doses.